Diamond and its olivine inclusions: a strange relation revealed by ab initio simulations.

(Article begins on next page)

23 April 2024

1 **Diamond and its olivine inclusions: a strange relation revealed by ab initio**

2 **simulations**

3 M. Bruno[1*], M. Rubbo[1], D. Aquilano[1], F.R. Massaro[2] & F. Nestola[2]

4

5 [1] Dipartimento di Scienze della Terra, Università degli Studi di Torino, Via Valperga Caluso 35, I-

6 10125 Torino, Italy

7 [2] Dipartimento di Geoscienze, Università degli Studi di Padova, Via Gradenigo 6, I-35131 Padova,

8 Italy

9

10 *Corresponding author
11 Email: marco.bruno@unito.it
12 Tel: +39 011 6705126
13 Fax: +39 011 6705128

14

15 **Abstract**

16 The study of diamond and its solid inclusions is of paramount importance to acquire direct

17 information on the deepest regions of the Earth. However, although diamond is one of the most

18 studied materials in geology, the diamond-inclusion relationships are not yet understood: do they

19 form simultaneously (syngenesis) or are inclusions pre-existing objects on which diamond

20 nucleated (protogenesis)?

21 Here we report, for the first time, adhesion energies between diamond (D) and forsterite (Fo) to

22 provide a crucial contribution to the syngenesis/protogenesis debate. The following interfaces were

23 investigated at quantum-mechanical level: (i) $(001)_D/(001)_{Fo}$, (ii) $(001)_D/(021)_{Fo}$, and (iii)

24 $(111)_D/(001)_{Fo}$. Our data, along with the ones recently obtained on the $(110)_D/(101)_{Fo}$ interface,

25 revealed an unexpected thermodynamic behaviour, all interfaces showing almost equal and low

26 adhesion energies: accordingly, diamond and olivine have an extremely low chemical affinity and

27 cannot develop preferential orientations, even during an eventual epitaxial growth. Combining these

28   results with those of our previous work concerning the morphology constraints of diamond on its

29   inclusions, we can state that the two main arguments used so far in favour of diamond/inclusions

30   syngenesis cannot be longer considered valid, at least for olivine.

31

32   **Key words**: diamond, olivine inclusion, epitaxy, syngenesis, protogenesis

33

34   **1. Introduction**

35   The characterization of mineral inclusions in diamond (D) allowed to indirectly obtain information

36   about the genesis and distribution of diamonds in the Earth's mantle (e.g., Pearson et al., 2014;

37   Shirey et al., 2013; Stachel and Harris, 2008). Such inclusions have been classified, according to the

38   timing of their formation with respect to the host diamond (Meyer, 1987; Harris, 1968a, 1968b), as:

39   (i) *syngenetic*: when they form simultaneously with the diamond; then, syngenesis implies either

40   inclusion/host mutual growth through co-precipitation from the same medium or complete

41   recrystallization of a pre-existing mineral occurring when diamond grows; (ii) *protogenetic*: when

42   they represent pre-existing minerals passively incorporated into the growing diamond; (iii)

43   *epigenetic*: when they are secondary minerals forming into a pre-existing diamond.

44   Determining whether an inclusion is syngenetic or protogenetic is of paramount importance

45   in diamond studies. Indeed, any geological information concerning a syngenetic inclusion (i.e.,

46   pressure and temperature of formation, age, geochemistry of the mother-medium) is applicable to

47   the host diamond: accordingly, a wrong interpretation concerning the genesis of the diamond-

48   inclusion couple could address to a misleading idea about the geological processes involved in the

49   diamond formation.

50   The most common proof invoked to establish if an inclusion is syngenetic lies in the

51   imposition of the morphology of the diamond on the inclusion (e.g., Sobolev, 1977; Harris, 1968a).

52   Such a traditional criterion is based on the belief that diamond can impose its cube-octahedral

53   morphology upon the inclusion only during their mutual growth. However, this is not supported by

2

54   any chemical-physical arguments, and even less by experimental evidences. Recently, the

55   morphologic criterion has been strongly criticized (Bruno et al., 2014; Nestola et al., 2014; Taylor

56   and Anand, 2004; Taylor et al., 2003). In particular, by analysing the diamond-imposed morphology

57   (Bruno et al., 2014) and the orientations (Nestola et al. 2014) of 43 olivine inclusions in 20

58   diamonds from the world-famous Udachnaya kimberlite in Siberia (Russia), the authors found that

59   many, if not most, olivine inclusions in diamonds are protogenetic and the diamond-imposed

60   morphology alone cannot be considered as a compelling proof of syngenesis of mineral inclusions

61   in diamonds.

62   The identification of an epitaxy, on the base of the orientation of the inclusion with respect

63   to its host (Pearson and Shirey, 1999; Harris and Gurney, 1979; Orlov, 1977; Sobolev, 1977), has

64   been considered as a further proof of syngenesis. Unfortunately, the only two works reporting a

65   statistically significant collection of data, have been recently published by Nestola et al. (2014) on

66   the Udachnaya diamonds and Neuser et al. (2015) on the Yubileinaya diamonds (Yakutia). In both

67   papers, the olivine inclusions were shown to be randomly oriented with respect to the hosting

68   diamond: Nestola et al. (2014) performed X-ray diffraction measurements, whereas Neuser et al.

69   (2015) carried out an EBSD analysis in order to determine the crystallographic orientations of the

70   inclusions. Previous works only reported limited sets of samples that are not sufficient to identify,

71   on a firm statistical ground, the mutual orientations between the crystallographic axes of the

72   inclusion and those of the host diamond (Frank-Kamenetsky, 1964; Futergendler and Frank-

73   Kamenetsky, 1961; Mitchell and Giardini, 1953). Moreover, the majority of these papers did not

74   consider the crystallographic contact planes (CCPs) defining the epitaxial interface. The latter

75   information is necessary to asses unambiguously a *preferential* epitaxial relationship since, on a

76   purely geometrical point of view, no constraints can be required on the contact plane of two

77   different phases with the same crystallographic orientation, the number of CCPs being potentially

78   infinite (Fig. S1, Supplementary Material). Indeed, if the inclusions do not show a systematic

79   preferential orientation with respect to diamond (random orientations), one is allowed to state that

80   there cannot be preferential epitaxial relationships, yet undefined. Conversely, the absence of

81   preferential orientation relationships is not sufficient to conclude that there is not an epitaxial

82   growth, as we will show in this work. Accordingly, it is evident that the *epitaxial criterion* to define

83   syngenesis can result rather ambiguous, if no information can be found on the thermodynamic

84   properties of the epitaxial interface.

85   Here, we focus on the study of the epitaxial phenomena in olivine-diamond system by an *ab*

86   *initio* quantum-mechanical computational approach, as such crystal features cannot be

87   experimentally investigated. Olivine forms a complete isomorphous series, with composition

88   ranging from forsterite (Mg_2SiO_4, Fo) to fayalite (Fe_2SiO_4, Fa). However, typical Earth's mantle

89   olivines are Mg-richer ($Fo_{92}Fa_8$) (e.g., Nestola et al., 2011). For this and for sake of simplicity, the

90   fayalite contribution in our model system was neglected. We investigated the $(001)_D/(001)_{Fo}$,

91    $(001)_D/(021)_{Fo}$, and $(111)_D/(001)_{Fo}$ epitaxial interfaces determining their structures and

92   thermodynamic properties. In detail, the specific adhesion energy $\beta^{D/Fo}_{(hkl)/(h'k'l')}$ (i.e., the energy gained,

93   per unit area, once the interface is formed) and the specific interface energy $\gamma^{D/Fo}_{(hkl)/(h'k'l')}$ (i.e., the

94   energy needed to create, per unit area, the interface), were calculated; (*hkl*) and (*h'k'l'*) define the

95   crystallographic faces in epitaxy of D and Fo, respectively. We decided to study the $(001)_D/(001)_{Fo}$,

96    $(001)_D/(021)_{Fo}$ and $(111)_D/(001)_{Fo}$ interfaces for two reasons: (i) the $(001)_D$, $(111)_D$, $(001)_{Fo}$ and

97    $(021)_{Fo}$ are important faces in the crystal morphology of diamond and olivine (e.g., Bruno et al.,

98   2014; De La Pierre et al., 2014); (ii) from a computational point of view, these systems are

99   workable with the resources of calculus actually in our hand.

100

101   **2. Calculation**

102   The calculations were performed with the *ab initio* CRYSTAL09 code (Dovesi et al., 2009; Dovesi

103   et al., 2005; Pisani et al., 1988) and at the DFT (Density Functional Theory) level with the B3LYP

104   Hamiltonian (Stephens et al., 1994; Becke, 1993; Lee et al., 1988), which provided accurate results

105   for the surface properties of the minerals considered in the present work (Bruno et al., 2014; De La

106   Pierre et al., 2014; Demichelis et al., 2015). Further computational details (e.g., basis set, thresholds

107   controlling the accuracy of the calculations) are given as Supplementary Material.

108   A composed slab (D/Fo/D), made by diamond (D) and forsterite (Fo) (slab D and slab Fo

109   hereinafter), was generated in the following way: (i) the two-dimensional (2D) coincidence lattices

110   between the two phases in epitaxial relationship were identified (Bruno et al. 2015); (ii) the slabs D

111   and Fo of a selected thickness were made by cutting their respective bulk structures parallel to the

112   *hkl* planes of interest and using the same 2D cell parameters describing the epitaxy; (iii) the slab Fo

113   was placed in between two slabs D; (iv) finally, the composed slab structure (atomic coordinates

114   and 2D cell parameters) was optimized by considering all the atoms free to move. The slab D/Fo/D

115   was generated preserving the symmetry centre, to ensure the vanishing of the dipole component

116   perpendicular to the slab. The CRYSTAL09 output files, listing the optimized fractional coordinates

117   and optimized 2D cell parameters of the composed slabs, are freely available at

118   http://mabruno.weebly.com/download. The calculations were performed by considering composed

119   slabs with a thickness sufficient to obtain an accurate description of the interfaces. The slab

120   thickness is considered appropriate when the bulk-like properties are reproduced at the centre of the

121   slabs D and Fo. Further details are given as Supplementary Material.

122   The specific adhesion energy, $\beta^{D/Fo}_{(hkl)/(h'k'l')}$ (J/m^2), is calculated by means of the relation:

123

124
$$\beta^{D/Fo}_{(hkl)/(h'k'l')} = \frac{E(2D) + E(Fo) - E(2D + Fo)}{2S} \quad (1)$$

125

126   where E(2D+Fo), E(2D) and E(Fo) are the static energies at 0K of the optimized slab D/Fo/D, slab

127   D/vacuum/D and slab Fo, respectively, and *S* is the area of the surface unit cell. Accordingly, the

128   surface energy is calculated:

129

130
$$\gamma^i_{(hkl)} = \frac{E(i) - E_b(i)}{2S} \; ; \; i = \text{D, Fo} \quad (2)$$

131

132   where $E_b(i)$ is the bulk energy of the *i*-th phase and the factor of 2 in the denominator accounts for

133   the upper and lower surfaces of the slab model.

134

135   **3. Results and discussion**

136   In Fig.1, the optimized structure of the $(001)_D/(001)_{Fo}$ interface is reported; the $(111)_D/(001)_{Fo}$ and

137    $(001)_D/(021)_{Fo}$ interfaces are given in Figs. S2 and S3 (Supplementary Material). A detailed

138   structural analysis of the interfaces is out of the scope of this work, therefore only a qualitative and

139   short description is given in the following. People interested to an in-depth structural analysis can

140   carry out it by using the CRYSTAL09 output file reporting the optimized atomic coordinates.

141   The significant structural modifications we observe at the three interfaces are not due to a strong

142   *chemical* interaction between the two phases, as it ensues from the comparison of the relaxed

143   structures of the surfaces in contact both with vacuum and the other mineral (Fig. 1 and Figs. S2-

144   S4). Indeed, the relaxation of the $(001)_D$ and $(111)_D$ surfaces in vacuum (De La Pierre et al., 2014)

145   only slightly differs from that observed when they are in contact with the (001) and (021) faces of

146   forsterite. To describe this geometry modification, we define the roughness of the carbon layer at

147   the interface with the parameter Δz (i.e., the difference between the z coordinates of the carbon

148   atoms within the same layer). Δz is 0.0206 Å for the carbon layer of the $(001)_D$ surface in vacuum,

149   whereas Δz is 0.2144 Å and 0.1712 Å for the carbon layer in contact with $(001)_{Fo}$ and $(021)_{Fo}$,

150   respectively. An analogous relaxation was reported by Bruno et al. (2015) for the $(110)_D$ surface: Δz

151   = 0.0038 Å for the carbon layer in vacuum and Δz = 0.1966 Å for the one in contact with $(101)_{Fo}$.

152   For the $(111)_D$ surface, the relaxation is smaller: Δz = 0.0028 and Δz = 0.0298 Å for that in vacuum

153   and in contact with $(001)_{Fo}$, respectively.

154   Similarly, the $(001)_{Fo}$ and $(021)_{Fo}$ surfaces are slightly affected by the presence of the diamond. The

155   strong distortion of the SiO_4 tetrahedra in proximity of the outmost diamond surfaces is analogue to

156   that found for the surface in vacuum. Majors differences are due to the distortion and rotation of

157   some SiO_4 tetrahedra to form C−O bonds in the $(001)_D/(001)_{Fo}$ and $(110)_D/(101)_{Fo}$ (Bruno et al.,

158   2015) interfaces.

159

160   **Table 1.** Optimized 2D cell parameters, adhesion and interfacial energies for the diamond/forsterite

161   epitaxies. The interfacial energies are calculated through Dupré's relation (e.g., Mutaftschiev, 2001)

162   and the following surface energy values: $\gamma_{(001)}^{D}$ = 4.820, $\gamma_{(111)}^{D}$ = 3.849, $\gamma_{(110)}^{D}$ = 5.046, $\gamma_{(001)}^{Fo}$ = 1.676,

163    $\gamma_{(021)}^{Fo}$ = 1.900 and $\gamma_{(101)}^{Fo}$ = 1.696 J/m^2. The data for the $(110)_D/(101)_{Fo}$ interface are from Bruno et al.

164   (2015).

interface	atoms	a (Å)	b (Å)	a^b (°)	area (Å^2)	β (J/m^2)	γ (J/m^2)
$(001)_D/(001)_{Fo}$	184	10.2382	4.9614	89.67	50.80	0.391	6.105
$(111)_D/(001)_{Fo}$	184	4.9899	9.9466	119.79	43.07	-0.934	6.459
$(001)_D/(021)_{Fo}$	304	4.9486	15.4411	89.95	76.41	0.243	6.477
$(110)_D/(101)_{Fo}$	280	7.4210	10.0444	90.09	74.54	0.367	6.375

165
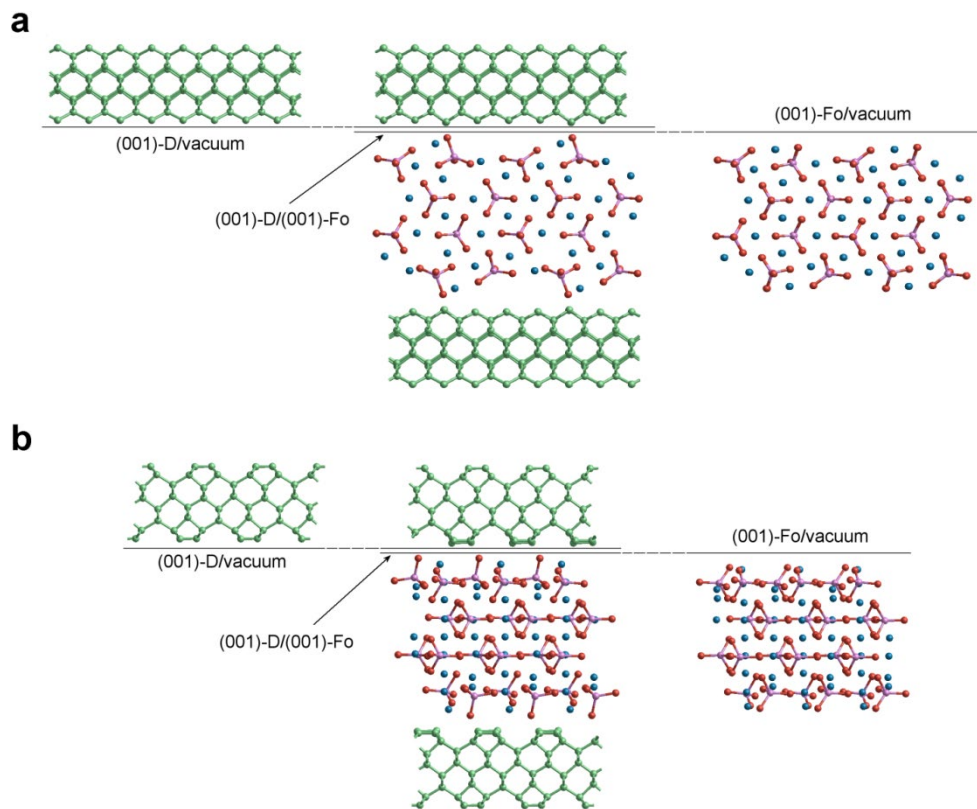
166

167   **Fig. 1.** Optimized $(001)_D/(001)_{Fo}$ (middle), $(001)_D$/vacuum (left) and $(001)_{Fo}$/vacuum interfaces

168   (right). The slabs are viewed along the (a) [110] and (b) [1$\overline{1}$0] directions of diamond. Mg, Si, O,

169   and C are blue, pink, red, and green, respectively. The black lines are a guide for eyes to indicate the

170   interfaces.

171

172   The weak interaction localized at the D/Fo interface can be ascribed to the extreme rigidity

173   of the diamond surfaces and to the noteworthy difference between the crystal fields belonging to the

174   two phases. Such structural incompatibility generates very low and similar values of the adhesion

175   energy (Table 1) for the $(001)_D/(001)_{Fo}$, $(001)_D/(021)_{Fo}$ and $(110)_D/(101)_{Fo}$ (Bruno et al., 2015)

176   interfaces, 0.243-0.391 J/m^2 (differences are within the calculation accuracy), and even a negative

177   one for the $(111)_D/(001)_{Fo}$ interface, -0.934 J/m^2. Interestingly, different values of $\beta_{(hkl)/(h'k'l')}^{D/Fo}$ provide

178   very similar values of $\gamma_{(hkl)/(h'k'l')}^{D/Fo}$ (Table 1) when the Dupré's relation (e.g., Mutaftschiev, 2001) is

179   used ($\gamma_{(hkl)/(h'k'l')}^{D/Fo} = \gamma_{(hkl)}^D + \gamma_{(h'k'l')}^{Fo} - \beta_{(hkl)/(h'k'l')}^{D/Fo}$), where $\gamma_{(hkl)}^D$ and $\gamma_{(h'k'l')}^{Fo}$ are the surface energies in the

180   vacuum of diamond and forsterite): 6.105-6.477 J/m^2. The implications of these findings are

181   numerous and outstanding. The epitaxy between the (111) face of diamond and forsterite results to

182   be very likely impossible. However, further calculations on epitaxial systems involving the $(111)_D$

183   and other forsterite surfaces could be performed to verify this statement. The (110) and (001) faces

184   of diamond show an undifferentiated behaviour with regard to forsterite; they seem to have the

185   same probability to make epitaxy with whatever surface of forsterite. According to the classical

186   nucleation theory (e.g., Mutaftschiev, 2001), lower the adhesion energy, lower the probability of the

187   3D-heterogeneous nucleation to occur (i.e., the formation of 3D nuclei of a phase A above a phase

188   B), the 3D-homogeneous nucleation becoming competitive as much as $\beta_{(hkl)/(h'k'l')}^{D/Fo}$ approaches to

189   zero. When $\beta_{(hkl)/(h'k'l')}^{D/Fo}$ is negative, as for the $(111)_D/(001)_{Fo}$ interface, a very peculiar case is spotted:

190   the homogeneous nucleation could occur more likely than the heterogeneous one.

191   An extremely interesting consequence of our calculations concerns the impossibility of the

192   diamond-forsterite system to develop a preferential orientation during any possible epitaxial growth.

193   This is in agreement with the recent crystallographic observations reported by Nestola et al. (2014)

194   and Neuser et al. (2015), where no overall preferred orientation of olivines in diamond was found. It

195   is evident that our results cast serious doubts on the application of the mere crystallographic

196   measurements of the relative orientations of diamond and olivine inclusions to hypothesize epitaxy

197   and, eventually, syngenesis. Indeed, if a preferential crystallographic orientation between inclusion

198   and host is not observed, this does not mean that the epitaxy cannot be realized; on the contrary,

199   epitaxy could occur through several D/Fo interfaces owing to the quasi-invariance of their adhesion

200   energy. Other silicate inclusions in diamond, with their outmost surfaces exhibiting SiO_4 tetrahedra,

201   like olivine, could show analogous behaviour. Preliminary measurements on orientation of garnet

202   inclusion in diamond (F. Nestola, personal communication), where a random distribution is

203   observed, seem to confirm such assumption.

204   Finally, from our findings on the quasi-invariance of the adhesion energies, the *epitaxial*

205   *criterion* alone results to be not adequate to discriminate between syngenesis and protogenesis in

206   the case of diamond-olivine pair. Three scenarios can be depicted to explain this concept. First, we

207   suppose a protogenetic origin for olivine: diamonds form from a carbon-rich fluid or melt

208   percolating homogeneously through an olivine-rich mantle rock (i.e., peridotite), by nucleating and

209   growing indifferently onto any olivine surfaces. Then, diamonds continue growing and fragments of

210   pre-existing olivine are entrapped. This represents a highly favorable scenario, since the mantle

211   rock is mainly composed by olivine and heterogeneous nucleation is always favored with respect to

212   the homogeneous one when $\beta_{(hkl)/(h'k'l')}^{D/Fo}$ is positive. Such a path should generate a rock containing

213   randomly oriented diamonds.

214   The second scenario accounts for a syngenetic origin of olivine inclusions: diamond nucleates

215   somewhere within the rock and, at a certain point of its history, olivines nucleate and grow on

216   diamond surfaces during its ongoing growth, without developing a preferential epitaxial

217   relationship, due to the quasi-invariance of $\beta_{(hkl)/(h'k'l')}^{D/Fo}$ values. Then, as for the protogenetic case, the

218   new formed olivines are entrapped in the growing diamonds without any preferential orientation.

219   In the last scenario, diamonds and olivines form through a homogeneous nucleation in the fluid.

220   Without an epitaxial control, no preferential crystallographic orientation can be developed: also in

221   this case, a rock having diamonds and its olivine inclusions with random orientations should be

9

222 obtained.

223 Summing up, no overall preferred orientation of olivines in diamond can be identified in a mantle

224 rock, both for syngenesis and protogenesis, as well as both in the case of heterogeneous and

225 homogeneous nucleation. Combining our results with those of Bruno et al. (2014) concerning the

226 morphology imposition by diamond on its inclusions, we can state that the two main arguments

227 playing in favour of syngenesis between diamond and its inclusions cannot be longer considered

228 valid. Alternative explanations must be provided to demonstrate the growth relationship between

229 diamond and its inclusions.

230

231 **4. Conclusions**

232 In this work, both the structure and energetics of the $(001)_D/(001)_{Fo}$, $(001)_D/(021)_{Fo}$, and

233 $(111)_D/(001)_{Fo}$ epitaxial interfaces were determined for the first time by means of *ab initio* quantum-

234 mechanical simulations. Our results can be summarized as follow:

235 (i) Diamond and forsterite have an extremely low chemical affinity: all interfaces show almost

236 equal and low adhesion energies.

237 (ii) From our findings on the quasi-invariance of the adhesion energies we can state that the

238 diamond-forsterite system is not able to develop a preferential orientation during any possible

239 epitaxial growth. Then, no overall preferred orientation of olivines in diamond can be identified in a

240 mantle rock.

241 (iii) The two main arguments in favour of syngenesis (i.e., morphologic and epitaxial criteria)

242 between diamond and its inclusions are not valid, at least for olivine. Alternative explanations must

243 be provided to demonstrate the growth relationship between diamond and its inclusions.

244 (iv) Other silicate inclusions (e.g., coesite, garnet, pyroxene) in diamond could show an analogous

245 behaviour to that of the olivine.

246 (v) It is important to highlight that we determined the adhesion energies by performing the

247 calculations at $T = 0K$ and $P = 0$. To take into accounts the effect of T and P on the adhesion energy

10

248 very demanding calculations should be done, which cannot be actually performed with the

249 computational resources at our disposal. Moreover, at the best of our knowledge, there are not

250 works in which the effect of *T* and *P* on the energetics of the epitaxial interfaces is discussed. This

251 lack of information prevents to know the behaviour of the adhesion energies when both

252 temperature and pressure increase. To have a realistic estimate of the effect of temperature for the

253 different diamond/forsterite interfaces, it is necessary to determine at *ab initio* level the frequencies

254 of the vibrational modes of the composed slabs, which are essential for calculating the vibrational

255 contribution (i.e., vibrational energy and vibrational entropy) to the interface energy of an epitaxial

256 system (e.g., Bruno, 2015; Bruno and Prencipe, 2013).

257 (vi) We performed the simulations by considering an olivine formed exclusively by the forsterite

258 end-member (Fo_{100}). Nevertheless, typical Earth's mantle olivines contain a small percentage of

259 iron ($\sim Fo_{92}Fa_8$), which could affect the values of the adhesion energies. Even in this case there are

260 not estimates of the effect of iron on the interaction between diamond and olivine. There is only a

261 very recent work (Navarro-Ruiz et al., 2014) where the authors calculated at *ab initio* level the

262 surface energy (at 0K and in the vacuum) of the (010) face of Mg-pure (Fo_{100}) and Fe-containing

263 ($Fo_{75}Fa_{25}$) olivines. The authors found that the (010) surface energy for $Fo_{75}Fa_{25}$ (0.870 J/m^2) is

264 lower by 25% than the (010) surface energy for Fo_{100} (1.160 J/m^2). This means that the iron has

265 certainly a strong effect on the values of the surface energy of the olivine faces and that it is licit to

266 expect that also the adhesion energies could be affected by the presence of fayalite. Hovever, since

267 the mantle olivines are poor in fayalite, it is likely that our estimates of adhesion energy values are

268 only slightly modified by the content of iron. Unless this latter tends to segregate preferentially onto

269 the crystal surfaces of olivine, by increasing the fayalite content at the diamond/olivine interface.

270 Such phenomenon was observed for Ca^{+2} in magnesium silicate olivine rich aggregates by Hiraga et

271 al. (2004) and energetically analysed by Alfredsson et al. (2005) for an orthorhombic $MgSiO_3$-

272 perovskite.

273 (vii) Another point to address is the following. We cannot state with absolute certainty that diamond

274 and olivine are in direct contact between them. It should be possible that a very thin layer (a few

275 Ångström thick?) of a fluid (or 2D solid) phase takes place in between diamond and olivine, so

276 forming a more complex interface. Obviously, only the experimental observation on natural samples

277 can give a definitive answer to such a question. It is sure yet that if a similar complex interface

278 exists, then the adhesion energies between diamond and olivine are completely different from those

279 determined in this work. It is for posterity to judge…

280

281 **References**

282 Alfredsson, M., Corà, F., Brodholt, J.P., Parker, S.C., Price, G.D., 2005. Crystal morphology and

283   surface structures of orthorhombic $MgSiO_3$ in the presence of divalent impurity ions. Phys.

284   Chem. Minerals 32, 379-387.

285 Becke, A.D., 1993. Density-functional thermochemistry. III. The role of exact exchange. J. Chem.

286   Phys. 98, 5648-5652.

287 Bruno, M., 2015. The free energy density of a crystal: calcite $(CaCO_3)$ as a case of study.

288   CrystEngComm, 17, 2204-2211.

289 Bruno, M., Rubbo, M., Pastero, L., Massaro, F.R., Nestola, F., Aquilano, D., 2015. Computational

290   approach to the study of epitaxy: natural occurrence in diamond/olivine and

291   aragonite/zabuyelite. Cryst. Growth Des. 15, 2979-2987.

292 Bruno, M., Massaro, F.R., Prencipe, M., Demichelis, R., De La Pierre, M., Nestola, F., 2014. Ab

293   initio calculations of the main crystal surfaces of forsterite (Mg_2SiO_4): a preliminary study to

294   understand the nature of geochemical processes at the olivine interface. J. Phys. Chem. C 118,

295   2498-2506.

296 Bruno, M., Prencipe, M., 2013. A new calculation strategy to analyze the vibrational free energy of

297   a slab and calculate the vibrational contribution of the surface free energy. CrystEngComm, 15,

298   6736-6744.

299 De La Pierre, M., Bruno, M., Manfredotti, C., Nestola, F., Prencipe, M., Manfredotti, C., 2014. The

300   (100), (110) and (111) surfaces of diamond: an ab initio B3LYP study. Mol. Phys. 112, 1030-

301   1039.

302   Demichelis, R., Bruno, M., Massaro, F.R., Prencipe, M., De La Pierre, M., Nestola, F.,2015. First-

303   principle modelling of forsterite surfaces properties: accuracy of methods and basis sets. J.

304   Comput. Chem. 36, 1439-1445.

305   Dovesi, R.,Saunders, V.R., Roetti, C., Orlando, R., Zicovich-Wilson, C.M., Pascale, F., Civalleri, B.,

306   Doll, K., Harrison, N.M., Bush, I.J., D'Arco, P., Llunell, M., 2009. CRYSTAL09 User's

307   Manual, University of Torino, Torino, Italy.

308   Dovesi, R., Orlando, R., Civalleri, B., Roetti, C., Saunders, V.R., Zicovich-Wilson, C.M.,

309   2005.CRYSTAL: a computational tool for the ab initio study of the electronic properties of

310   crystals. Z. Kristallogr. 220, 571-573.

311   Frank-Kamenetsky, V.A., 1964. The nature of structural impurities and inclusions in minerals. Gos.

312   Univ., Leningrad. [In Russian].

313   Futergendler, S.I., Frank-Kamenetsky, V.A., 1961. Oriented inclusions of olivine, garnet and

314   chrome-spinel in diamonds. Zapisky Vsesoyuznogo Mineralogicheskogo Obshestva 90, 230-

315   236. [In Russian].

316   Harris, J.W., Gurney, J.J., 1979.In: Field, J.E. (Ed.), Properties of diamond. Academic Press,

317   London, pp. 555-591.

318   Harris, J.W., 1968a. The recognition of diamond inclusions. Pt. 1: Syngenetic inclusions. Industrial

319   Diamond Reviews 28, 402-410.

320   Harris, J.W.,1968b. The recognition of diamond inclusions. Pt. 2: Epigenetic inclusions. Industrial

321   Diamond Reviews 28, 458-461.

322   Hiraga, T., Anderson, I.M., Kohlstedt, D.L., 2004. Grain boundaries as reservoirs of incompatible

323   elements in the Earth's mantle. Nature 427, 699-703.

324   Lee, C., Yang, W., Parr, R.G., 1988. Development of the Colle-Salvetti correlation-energy formula

325   into a functional of the electron density. Phys. Rev. B 37, 785-789.

326 Meyer, H.O.A., 1987. In: Nixon, P.H. (Ed.), Mantle xenoliths. John Wiley & Sons, Chichester, pp.

327   501-522.

328 Mitchell, R.S., Giardini, A.A.. 1953. Oriented olivine inclusions in diamond. Am. Mineral. 38, 136-

329   138.

330 Mutaftschiev, B., 2001. The Atomistic Nature in Crystal Growth. Springer Series in Materials

331   Science. Springer-Verlag, Berlin, 368 pp.

332 Navarro-Ruiz, J., Ugliengo, P., Rimola, A., Sodupe, M., 2014. B3LYP periodic study of the

333   physiochemical properties of the nonpolar (010) Mg-pure and Fe-containing olivine surfaces. J.

334   Phys. Chem. A 118, 5866-5875.

335 Nestola, F., Nimis, P., Angel, R.J., Milani, S., Bruno, M., Prencipe, M., Harris, J.W., 2014. Olivine

336   with diamond-imposed morphology included in diamond. Syngenesis or protogenesis?

337   International Geology Review 56, 1658-1667.

338 Nestola, F., Nimis, P., Ziberna, L., Longo, M., Marzoli, A., Harris, J.W., Manghnani, M.H.,

339   Fedortchouk, Y., 2011. First crystal-structure determination of olivine in diamond: Composition

340   and implications for provenance in the Earth's mantle. Earth Planet. Sci. Lett. 305, 249-255.

341 Neuser, R.D., Schertl, H.-P., Logvinova, A.M.,Sobolev, N.V., 2015. An EBSD study of olivine

342   inclusions in Siberian diamonds: evidence for syngenetic growth? Russian Geology and

343   Geophysics 56, 321-329.

344 Orlov, Y.L., 1977. The mineralogy of the diamond. John Wiley & Sons, New York, 235 pp.

345   [Translation of Mineralogiiaalmaza, Izdatel'stva Nauka, 1973, in Russian].

346 Pearson, D.G., Brenker, F.E., Nestola, F., McNeill, J., Nasdala,L., Hutchison, M.T., Matveev, S.,

347   Mather, K., Silversmit, G., Schmitz, S., Vekemans, B., Vincze, L., 2014. Hydrous mantle

348   transition zone indicated by ringwoodite included within diamond. *Nature* **507**, 221-224.

349 Pearson, D.G., Shirey, S.B., 1999. In: Lambert, D.D., Ruiz, J.(Eds.), Application of radiogenic

350   isotopes to ore deposit research and exploration. Society of Economic Geologists, Boulder,

351   Colorado, pp. 143-171.

352 Pisani, C., Dovesi, R., Roetti, C., 1988. Hartree-Fock ab-initio treatment of crystalline systems.

353 Lecture Notes in Chemistry. Springer-Verlag, Berlin, 195 pp.

354 Shirey, S.B., Cartigny, P., Frost, D.J., Keshav, S., Nestola, F., Nimis, P., Pearson, D.G., Sobolev,

355 N.V., Walter, M.J., 2013. Diamonds and the geology of mantle carbon. Rev. Min. Geochem.75,

356 355-421.

357 Sobolev, N.V., 1977. Deep-seated inclusions in kimberlites and the problem of the composition of

358 the upper mantle. American Geophysical Union, Washington, D.C., 279 pp.

359 Stachel, T., Harris, J.W., 2008. The origin of cratonic diamonds-constraints from mineral inclusions.

360 Ore Geol. Rev. 34, 5–32.

361 Stephens, P.J., Devlin, F.J., Chabalowski, C.F., Frisch, M.J., 1994. Ab initio calculation of

362 vibrational absorption and circular dichroism spectra using density functional force fields. J.

363 Phys. Chem. 98, 11623-11627.

364 Taylor, L.A., Anand, M., Promprated, P., 2003. Diamonds and their inclusions: are the criteria for

365 syngenesis valid? Eighth International Kimberlite Conference, Extended Abstract, Victoria,

366 Canada, 1-5.

367 Taylor, L.A., Anand, M., 2004. The origin of diamonds: time capsules from the Siberian Mantle,

368 2004. Chem. Erde 64, 1-74.

369

370 **Acknowledgments**

375